# Multi-Mode Operations for On-line Uninterruptible Power Supply

Jinghang Lu, Mehdi Savaghebi,Yajuan Guan, Mingshen Li, and Josep Guerrero
Department of Energy Technology
Aalborg University
Aalborg, Denmark
{jgl, mes,ygu,msh,joz}@et.aau.dk

***Abstract*—In this paper, the multi-mode operation of the on-line UPS system is investigated and corresponding control strategies are proposed. The proposed control strategies are able to achieve the seamless transition in traditional normal mode, PV-aided normal mode, enhanced eco-mode and burn-in test mode. At the same time, the uninterruptible load voltage is guaranteed during the transition between these modes. Furthermore, the stability of enhanced eco-mode and burn-in test mode is studied by small signal analysis. Finally, extensive experimental results are provided to validate the effectiveness of the proposed methods.**

***Keywords—Burn-in test mode; Enhanced eco-mode; PV-aided normal mode; Seamless transfer; Uninterruptible Power Supply (UPS);***

## I. INTRODUCTION

Over the last few years, Uninterruptible Power Supply (UPS) system has been widely installed in the communication systems, network centers, financial institution and medical equipment to provide conditioned and reliable power [1, 2]. According to the IEC Standard 62040-3 [3], the UPS system is categorized as on-line, off-line, and line-interactive UPS systems in the normal mode of operation. The on-line UPS system is commonly configured for sensitive loads among them, as it isolates the load from the grid that may suffer from grid frequency variation and voltage irregularity. A conventional on-line UPS system consists of AC/DC, DC/AC, a battery bank, and a static bypass switch [4]. To provide more redundancy in the system and supply more reliable power, parallel inverter modules are connected to deliver the power to the sensitive loads as shown in Fig.1 [5].

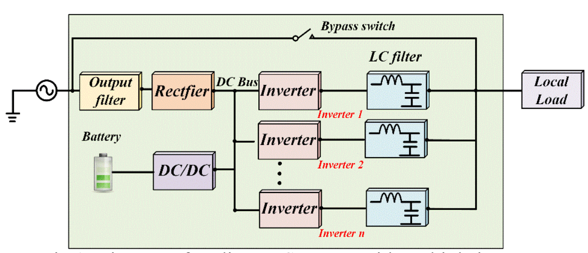

Fig.1. Diagram of on-line UPS system with multiple inverters

In the traditional normal mode of operation in the on-line UPS system, load power is provided by the combination of AC/DC and DC/AC converters. Recently, some studies have been conducted by integrating fuel cell, or multiple renewable energy sources into the UPS system [6-9], which claims to improve the performance of UPS system under normal and backup mode of operation. Among these studies, [9] proposed a seamless transfer control strategy for fuel cell-based UPS system. However, considering the slow dynamics, high cost of the fuel cell, it may not be quite suitable for the on-line UPS system. The works of [6-8] proposed a super UPS topology, where the fuel cell, supercapacitor, PV, and gas turbine are all integrated into the UPS system. However, incorporating all these energy units into the UPS system inevitably increase the client's economic burden and it is quite complicated and challenging for the energy management of the super UPS system. Therefore, only incorporating the PV unit into the UPS system may be a promising solution, as the priority of employing the solar energy reduces the cost of the electricity from the grid. Moreover, it is eco-friendly generation. Hence, the PV-aided normal mode (PNM) of on-line UPS system can improve the overall system performance considering better economic and environmental benefits.

However, if the PV system is unavailable or at low efficiency, i.e. during the night, the operation of the on-line UPS system has to return to the traditional normal mode (TNM). To save more energy, the eco-mode operation of the UPS system has been recently proposed by several UPS manufacturers [10, 11], the eco-mode operation is similar to the normal operation in off-line UPS system, where the load is directly powered by the grid through the bypass switch and the inverters is operated in "standby" mode as shown in Fig.2. The eco-mode shows the benefits that the efficiency of the power delivery through the bypass path is typically between 98% to 99%, compared to 94%-97% of the TNM operation in on-line UPS system. Nonetheless, usually, UPS system provides both active and reactive power to the load. If the UPS operates in traditional eco-mode, the grid typically charges extra fees for delivering the reactive power to the load. Therefore, the Active Eco-mode (AEM) or Improved Eco-mode concept is proposed by the UPS manufacturers [10, 11], which means that the active power of the load is provided by the grid and its reactive power is supplied by the UPS system. For instance, [12] proposed an AEM by current control of inverters. However, the transition for the inverter from the voltage controlled mode to the current controlled mode inevitably takes quite a long time. And it significantly affects the

978-1-5386-1180-7/18/$31.00 ©2018 IEEE

smooth transition between TNM and AEM. Therefore, an enhanced eco-mode (EEM) control strategy should be investigated to make sure that the inverters are always controlled in Voltage Control Mode (VCM) when the UPS operation mode shifts between the TNM and the EEM. In this way, the seamless transition from TNM to EEM is guaranteed so that the output voltage under transition is not affected.

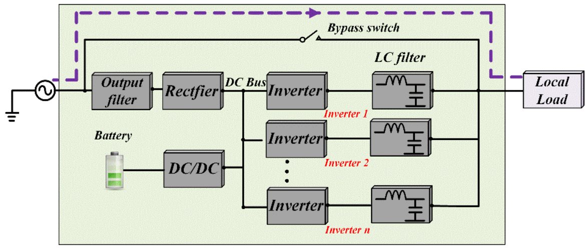


Fig.2. Traditional Eco-mode of on-line UPS system

In addition, the new UPS system needs to do the burn-in test for the quality certification. Traditionally, in the burn-in test mode (BTM), the output of the UPS system is connected with the resistor bank. Consequently, unwanted energy consumption caused by the resistor bank leads to the cost increase for the UPS manufacturers. Therefore, the energy saving methods are considered to be important for the UPS manufacturers. Until now, the energy saving methods in the burn-in test mode have been proposed by [13-15]. In [14], an inductor and a transformer are connected between the output of the UPS system and the grid. However, the passive, bulky and heavy equipment is quite inconvenient for burn-in test. To overcome the drawback, current-controlled inverter [13] and open-loop voltage-controlled inverters [15] have been suggested to replace the passive equipment. However, these control strategies are either too complicated or trigger the harmonics propagation. Moreover, inverter modules of the UPS system are usually controlled in VCM in the normal mode of operation. When the current controlled inverter is implemented for the BTM, it is difficult to achieve the seamless transition between the TNM and the BTM. Therefore, a voltage-controlled inverter for the BTM and the seamless transition between TNM and BTM needs to be investigated.

In this paper, the multi-mode operations of the on-line UPS system is investigated and the seamless transfer control strategy is proposed. Especially, the control strategy for TNM, PNM, EEM and BTM are proposed for the on-line UPS system, and the seamless transfer achieved as well. Small signal analysis is conducted to investigate the stability of the EMM and BTM. Experimental results are provided to validate the effectiveness of the proposed methods.

## II. MULTI-MODE OPERATION FOR THE ON-LINE UPS SYSTEM

As mentioned in the previous section, the operation of the on-line UPS system can be divided into TNM, PNM, EEM and BTM when the grid is normal. The details of the operation in these modes are illustrated in the following parts of this section.

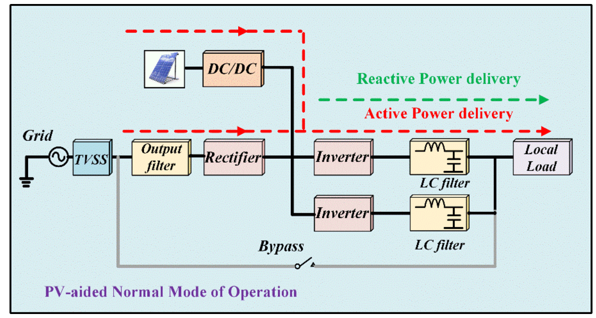


Fig.3. Power Flow in the normal mode of operation in PV-aided On-line UPS system

### *A. Normal Mode*

In the TNM operation of the on-line UPS system, the load power is provided by the combination of AC/DC and DC/AC converters (rectifier and inverter, respectively). When the PV system is incorporated in the on-line UPS system, the load power is supplied by the combination of the PV system, rectifier and inverter as shown in Fig.3. It should be noted that the battery has been charged to full SoC and operate in standby mode, so it does not involve in the power supply to the load in the normal mode. From the point of saving the electricity purchase from the grid, the PV panel should always be working in MPPT mode to generate maximum available power. The extra required active power is provided by the grid through the AC/DC and DC/AC converters.

*1) Control strategy for DC/AC inverters in on-line UPS system*

Fig.4 shows the control strategy of the UPS system in the PNM operation. The robust AC/DC control strategy that was proposed by [16] has been implemented in this paper. For the parallel operation of the inverter modules, the droop control strategy is implemented. Due to the short distance from the UPS system to the load, the line impedance is considered to be negligible. Therefore, a virtual resistance $R_v$ is embedded in the control diagram to force the output line impedance to be resistive (see Fig.4). As the output impedance is mainly resistive, the $Q\sim\omega$, $P\sim E$ droop control strategy is implemented in the control loop, as shown in the expression:

$$\omega = \omega^* + D_q Q_{LPF} \tag{1}$$

$$E = E^* - D_p P_{LPF} \tag{2}$$

where $\omega^*$ and $\omega$ are the inverter nominal and reference frequency. $E^*$ and $E$ are the inverter nominal and reference voltage magnitude. $D_p$ and $D_q$ are the droop coefficients for controlling the output active power $P_{LPF}$ and reactive power $Q_{LPF}$, respectively. $P_{LPF}$ and $Q_{LPF}$ are calculated as:

$$P_{LPF} = \frac{3}{2(\tau s+1)}(V_{c\alpha}I_{o\alpha} + V_{c\beta}I_{o\beta}) \tag{3}$$

$$Q_{LPF} = \frac{3}{2(\tau s+1)}(V_{c\beta}I_{o\alpha} + V_{c\alpha}I_{o\beta}) \tag{4}$$

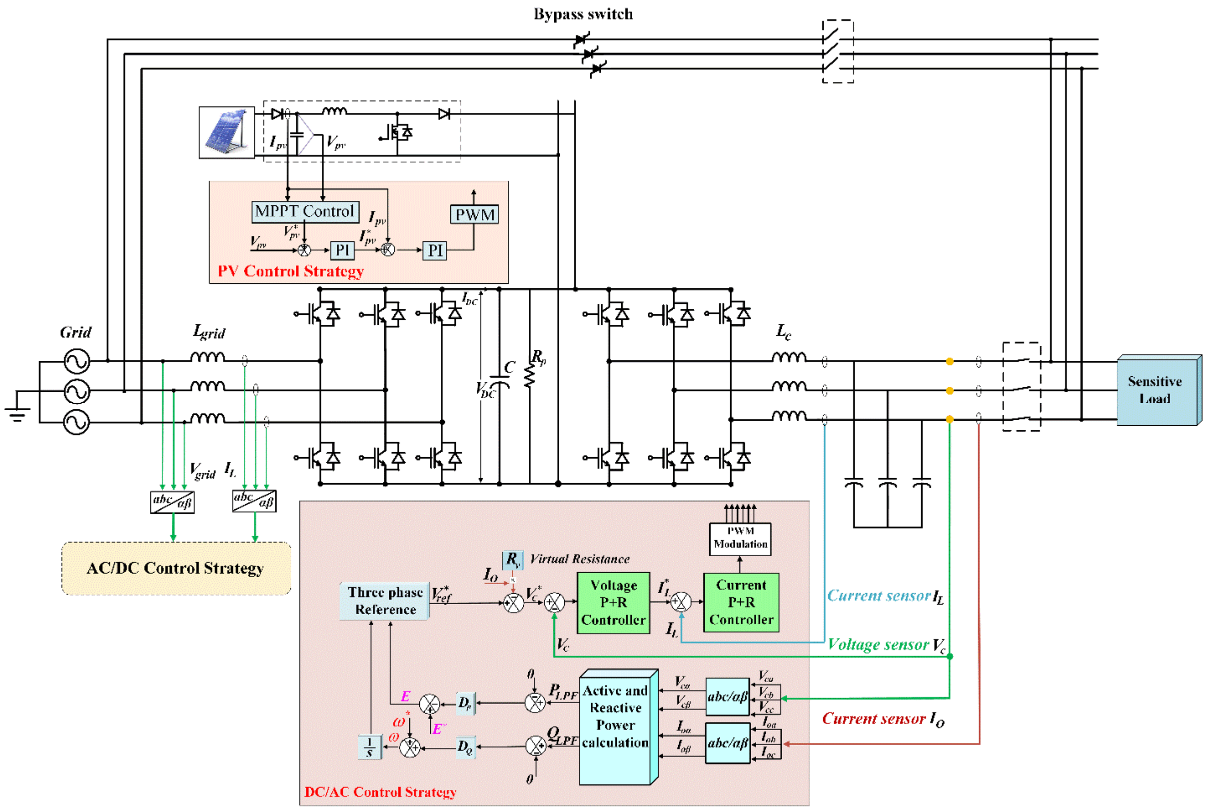

Fig.4. Control strategy of PV-aided On-line UPS system in normal mode of operation.

where $\tau$ is the time constant of the low-pass filter. $V_{c\alpha}$ and $V_{c\beta}$ are the output voltage through Clarke transformation. $I_{o\alpha}$ and $I_{o\beta}$ are the output current through Clarke transformation.

In addition, in order to achieve voltage tracking, a dual loop strategy with outer voltage Proportional Resonant (P+R) control and inner current P+R control strategy are adopted in the paper. The outer loop regulates the output capacitor's voltage and inner loop controls the inverter side current. These controllers are as follows:

$$G_v(s) = k_{pv} + \frac{k_{rV} s}{s^2+(\omega_o)^2} \quad (5)$$

$$G_i(s) = k_{pi} + \frac{k_{ri} s}{s^2+(\omega_o)^2} \quad (6)$$

where $k_{pv}$ and $k_{pi}$ are the proportional terms, $k_{rV}$ and $k_{ri}$ are the resonant term coefficient at $\omega_o = 314rad/s$. The inner current loop is designed to provide sufficient damping and protect the inductor from overcurrent.

*2) PV energy and control system*

Normally, the PV panel is operated in MPPT mode as shown in Fig. 4, where the power of the PV panel is expressed as:

$$P_{pv} = V_{pv} I_{pv} \quad (7)$$

where $V_{pv}$ and $I_{pv}$ are the voltage and current at the terminal of the PV panel. Several MPPT algorithm such as : perturb and observe method can be applied into the system to extract the maximum power. Moreover, in order to regulate the PV output voltage and prevent PV output overcurrent, the double loop PI controller is adopted in the system (Fig.4). It should be pointed out that the complex algorithm of MPPT is not discussed here as it is beyond the scope of this paper.

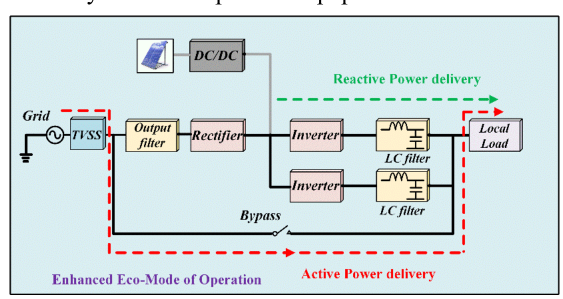

Fig.5. Power flow of Enhanced Eco-mode in the On-line UPS system

## B. *Enhanced Eco mode and seamless transition*

When the PV system is unavailable, The UPS system operation mode may transfer from the TNM to the EEM, where the active power is directly powered by the grid, meanwhile, the reactive power of the load is provided by the inverter as shown in Fig.5. Moreover, the transition from EEM to the TNM and

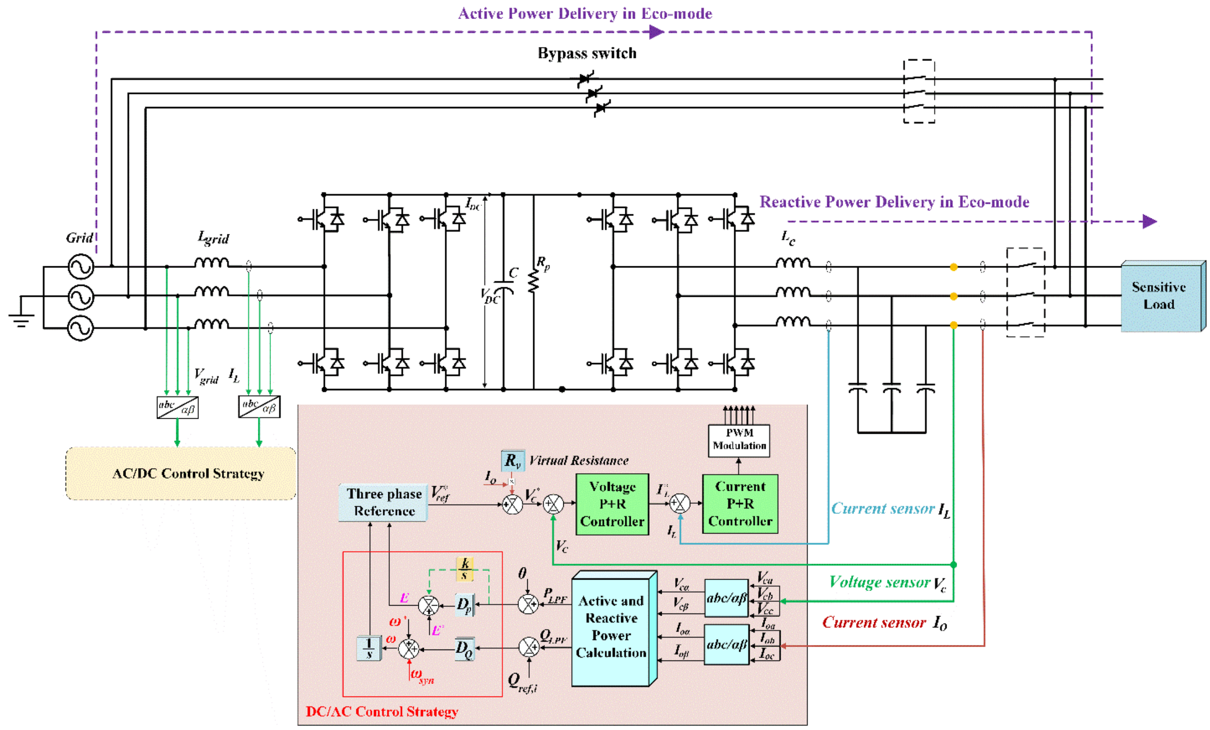


Fig.6. The control Strategy of the EEM operation in operation in the on-line UPS system.

vice versa should be seamless, in other words, the UPS output voltage should not have abrupt amplitude or frequency changes during the transition.

The proposed control strategy for EEM operation is shown in Fig.6. In the EEM, the output active power of the UPS system should be zero, in order to make sure the zero steady state active power tracking, the integral term $\frac{K}{s}$ is added in the $P\sim E$ droop control strategy; meanwhile, the reactive power reference is determined by calculating the total load reactive power. If multiple inverters together provide the reactive power, the reactive power reference for each inverter should be $Q_{ref,i}=\frac{1}{N}Q_{Load}$. So, the droop control strategy in EEM is expressed as:

$$\mathrm{E}=\mathrm{E}^{*}+D_p(0-P_{LPF})+\frac{K}{s}(0-P_{LPF}) \quad (8)$$

$$\omega=\omega^{*}+D_Q\left(Q_{ref}-Q_{LPF}\right)+\omega_{syc} \quad (9)$$

## C. Burn-in Test mode

The power flow in the burn-in test is shown in Fig.7. Specifically, at no load condition (see Fig.7 (a)), the active power drawn from the grid is fed back again through the bypass switch. On the contrary, when the local load is connected to the UPS system, the power flow is shown in Fig. 7(b), where the active power drawn from the grid flows to the local load and is delivered back to the grid, respectively.

The proposed control strategy is expressed as:

$$\mathrm{E}=\mathrm{E}^{*}+D_p\left(P_{ref}-P_{LPF}\right)+\frac{k}{s}\left(P_{ref}-P_{LPF}\right) \quad (10)$$

$$\omega=\omega^{*}-D_Q\left(Q_{ref}-Q_{LPF}\right)+\omega_{syc} \quad (11)$$

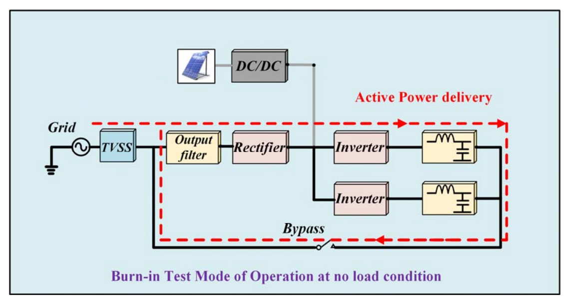


(a)

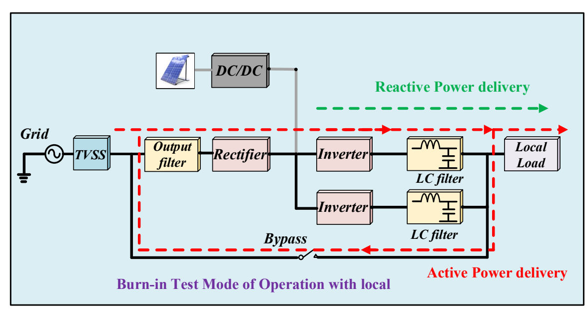


(b)

Fig.7. Burn-in test mode of operation for On-line UPS system (a) no

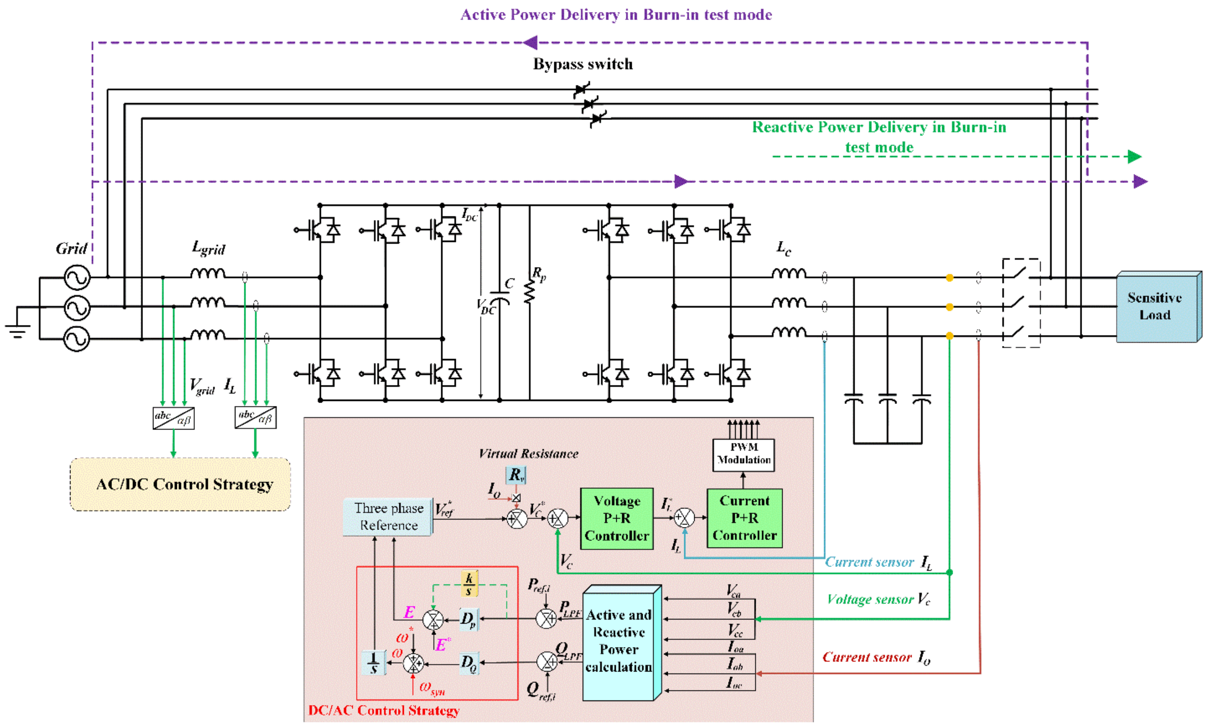


Fig.8. The control Strategy of the BTM operation in operation in the on-line UPS system.

where $P_{ref}$ and $Q_{ref}$ is the reference active and reactive power that needs to be delivered to the grid by the inverters. It is noted that in order to ensure the zero steady state active power tracking, the integral term $\frac{K}{s}$ is added in the P$\sim E$ droop control strategy, meanwhile, the reactive power reference is determined by calculating the total load reactive power. In addition, under light load or no load condition, $Q_{ref} = 0$. Meanwhile, it is found that the control strategy in Eco-mode is very similar as the Burn-in test mode. The operation mode can be easily switched from one mode to another by changing the reference value of the droop control. In this way, the seamless transfer between different modes can be realized without affecting the output voltage of the UPS system.

## III. STABILITY ANALYSIS

From the discussions in Section II.B and II.C, it is observed that the EEM and the BTM can be achieved with the same control strategy by adjusting different reference values. Therefore, in this section, the system small-signal stability of EEM and the BTM operations is investigated. First, the power flow of the UPS system through a general line impedance is obtained as [17]:

$$P = \left(\frac{EV}{Z}\cos(\varphi) - \frac{V^2}{Z}\right)\cdot\cos(\theta) + \frac{EV}{Z}\sin(\varphi)\sin(\theta) \quad (12)$$

$$Q = \left(\frac{EV}{Z}\cos(\varphi) - \frac{V^2}{Z}\right)\cdot\sin(\theta) - \frac{EV}{Z}\sin(\varphi)\sin(\theta) \quad (13)$$

where $P$ and $Q$ are the instantaneous active and reactive powers of the UPS system. $E$ and $V$ are the amplitudes of the inverter output voltage and the common bus voltage, respectively, and $\varphi$ is the power angle. $Z$ and $\theta$ are the magnitude and phase of the output impedance, respectively.
Considering that the line impedance most often demonstrates a resistive characteristic in the UPS applications, the power flow of the UPS system can be expressed as:

$$P = \frac{V}{R}(E\cos(\varphi) - V) \cong \frac{V}{R}(E - V) \quad (14)$$

$$Q = -\frac{EV}{R}\sin(\varphi) \cong -\frac{EV}{R}\varphi \quad (15)$$

Accordingly, the active and reactive power variation according to the UPS voltage amplitude and phase angle disturbance can be obtained by:

$$\Delta P = \left(\frac{\partial P}{\partial E}\right)\Delta E + \left(\frac{\partial P}{\partial \varphi}\right)\Delta\varphi = k_{PE}\Delta E + k_{P\varphi}\Delta\varphi \quad (16)$$

$$\Delta Q = \left(\frac{\partial Q}{\partial E}\right)\Delta E + \left(\frac{\partial Q}{\partial \varphi}\right)\Delta\varphi = k_{QE}\Delta E + k_{Q\varphi}\Delta\varphi \quad (17)$$

where the operator $\Delta$ indicates a small-signal perturbation around the UPS's operating equilibrium point.

When there are some power fluctuation during the EEM or the BTM, expanding the proposed control strategy in (8)-(9) or (10)-(11) results in the small signal responses of the UPS voltage, which are expressed as:

$$\Delta E = -D_P \Delta P_{LPF} - \frac{k}{s}\Delta P_{LPF} \quad (18)$$

$$\Delta\omega = D_Q \Delta Q_{LPF} \quad (19)$$

$$\Delta P_{LPF} = \frac{1}{\tau s + 1}\Delta P \quad (20)$$

$$\Delta Q_{LPF} = \frac{1}{\tau s + 1}\Delta Q \quad (21)$$

where $\tau$ is the time constant of the low-pass filter in the active and reactive power calculation.

Considering that $\Delta\theta = \frac{1}{s} \cdot \Delta\omega$, and by the simple manipulation of (16)-(21), the dynamic performance of the UPS system in the EEM or BTM operation yields the following expression:

$$(M_{2\times2} - N_{2\times2} \cdot L_{2\times2}) \cdot [\Delta E;\ \Delta\varphi]^T = 0 \quad (22)$$

where $M_{2\times2} = \begin{bmatrix} s(\tau s+1) & 0 \\ 0 & s(\tau s+1) \end{bmatrix}$,

$$N_{2\times2} = \begin{bmatrix} -(D_P s + k) & 0 \\ 0 & D_Q \end{bmatrix},\ L_{2\times2} = \begin{bmatrix} k_{PE} & k_{P\varphi} \\ k_{QE} & k_{Q\varphi} \end{bmatrix}$$

The eigenvalues of (22) show the small-signal response of the UPS system during EEM and BTM. In addition, note that when $k$=0, the matrix $N_{2\times2}$ is expressed as:

$$N_{2\times2} = \begin{bmatrix} -D_P s & 0 \\ 0 & D_Q \end{bmatrix} \quad (23)$$

The matrix of (23) indicates the behavior of the UPS system in TNM and PNM operation.

The performance of the system with different values of $k$ is evaluated and shown in Fig.9. With UPS system parameters listed in the Table I, Fig.9 shows the root locus of the proposed control strategy, where the droop control coefficient is fixed while the parameter $k$ varies from 0.0033 to 0.0213. As illustrated, it is a fourth-order system and dynamic performance is mainly determined by the dominant poles of $\lambda_1$ and $\lambda_4$. It can be observed that when $k$ is increased from 0.0033 to 0.0213, the system stability is improved but an underdamped response is observed. Therefore, the selection of parameter $k$ involves a trade-off between the system stability and damping response. In order to obtain satisfied satisfactory damping and stability performance, the parameter $k$ is selected as 0.007.

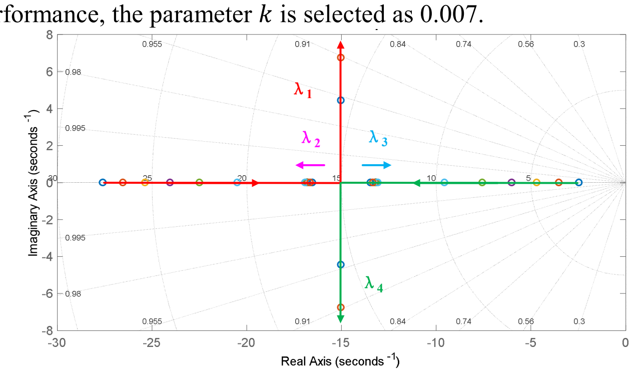


Fig.9. Root Locus with the proposed control strategy when the parameter changes: $0.0033 < k < 0.0213$

TABLE I. SYSTEM AND CONTROLLER PARAMETERS

| | |
|---|---|
| System Parameters | |
| Filter Inductor $L_f$ | $1.8mH$ |
| Normal DC link Capacitor | $0.011F$ |
| Sampling frequency $f_s$ | 10kHz |
| Electrical Parameter of the AC/DC and DC/AC Converter | |
| Converter Rating | 1kVA |
| Phase-to-phase RMS Voltage | 208V |
| Peak phase current | 4.4A |
| DC link voltage | 500V |
| Droop Coefficient | |
| Frequency droop $D_q$ | 0.0001 |
| Voltage droop $D_p$ | 0.00005 |
| Integral term $k$ | 0.007 |
| Voltage Control Parameter | |
| Proportional gain$K_{pv}$ | 0.2 |
| Resonant gain $K_{iv}$ | 100 |
| Current controller Parameter | |
| Proportional gain$K_{pi}$ | 8 |
| Resonant gain $K_{ii}$ | 500 |

## IV. EXPERIMENTAL RESULTS

In order to validate the feasibility of the proposed multi-mode operation of the on-line UPS system, the system diagram shown in Fig.4 is built up and shown in Fig.10. The setup consists of an AC/DC converter, a DC/AC converter, a PV emulation unit and a bypass switch. The DC bus is formed by the DC-link capacitors. The control algorithm is implemented in dSPACE 1006 platform for real-time control. System parameters are listed in Table I. Waveforms are captured by an oscilloscope

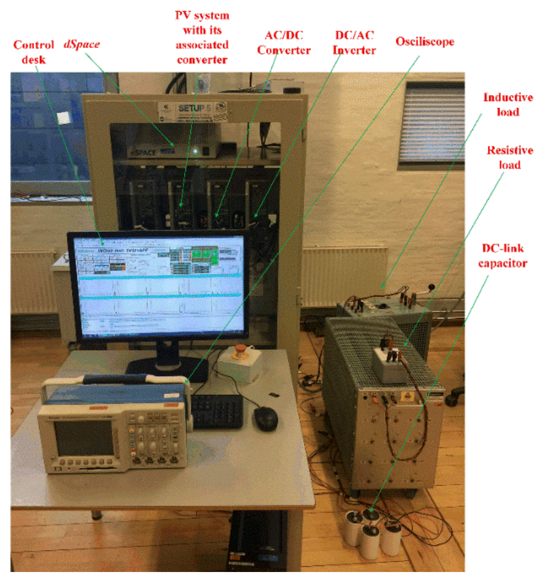


Fig.10. Configuration of the setup

### *A. Transition between TNM and PNM operation of the on-line UPS system*

In this section, the schematic diagram with the proposed control strategy in Fig.4 is tested with the setup in Fig.10. Fig.11 shows the active and reactive power waveforms between the TNM and the PNM operation. As can be observed in Fig.18????, the load active and reactive powers are respectively $P_{load}$=700W and $Q_{load}$ =120Var. At the TNM operation, the active power delivered from the grid is $P_{in} = 800W$ (blue waveform). Note that the difference between $P_{in}$ and $P_{load}$ is caused by the power loss in the UPS system. When the operation mode shifts to the PNM from TNM, the PV output active power is 250W (cyan waveform), so the active power delivery from the grid drops to the 550W. When the PV is unavailable, the UPS system returns to the TNM again, and the active power delivery from the grid increases to 800W, as shown in Fig.11. Meanwhile, it is observed that the load active power and reactive power (green waveform and purple waveform) do not change during the transition. Finally, the load voltage waveform during the transition is shown in Fig.12, where it can be seen that this voltage is uninterruptible during the transition.

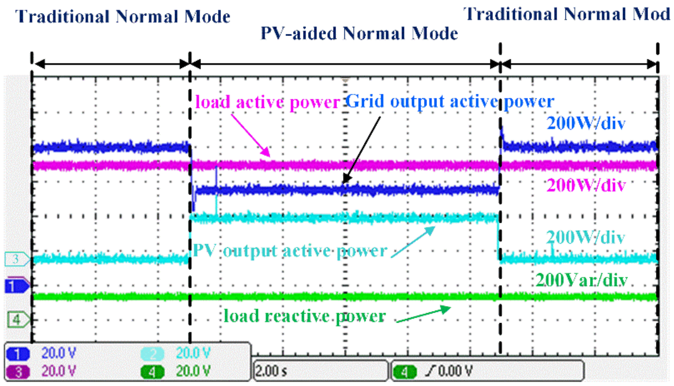

Fig.11. Active and reactive power in transfer between TNM and PNM operation.

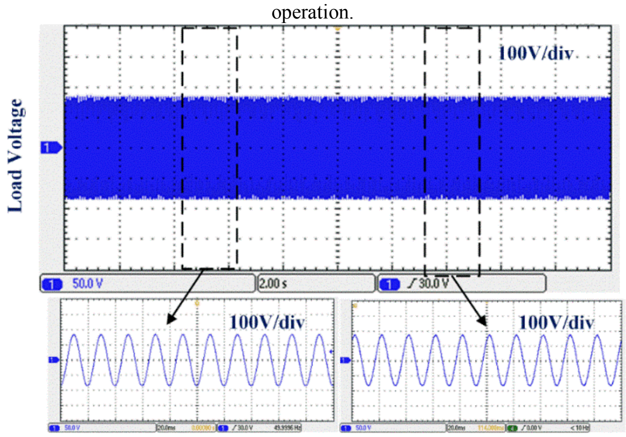

Fig.12. Load voltage in transfer between between TNM and PNM operation

## *B. Transition between TNM and EEM operation of the on-line UPS system*

In this test, the seamless transition between the TNM and the EEM is evaluated. As shown in Fig. 13(a), when the operation mode of the UPS shifts from TNM to EEM, the load active power provided by the inverter drops to zero (blue waveform), and the 520W active power is directly provided by the grid through the bypass switch (purple waveform). Meanwhile, the reactive power is still powered by the inverter (cyan waveform). On the contrary, when the operation mode of the UPS shifts from the EEM to the TNM, the load active power is delivered from the inverter and the active power goes through the bypass switch decreased to zero. Figs.13 (b) and (c) show the load voltage waveforms during the transition, it is indicated that the load voltage is uninterruptible and the whole transition is seamless.

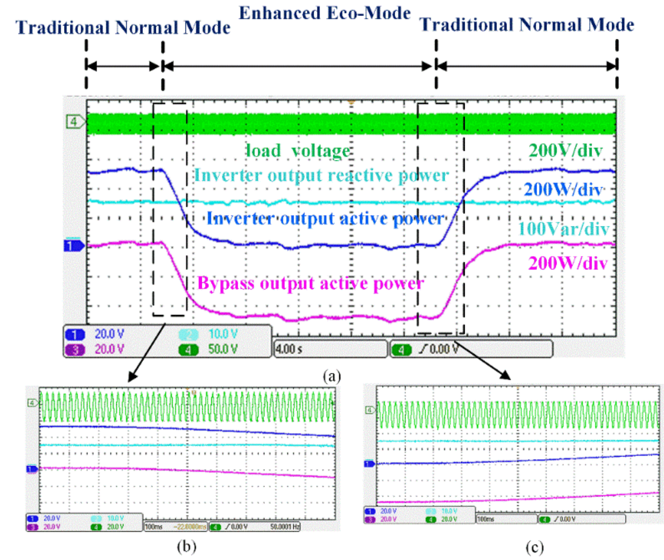

Fig.13. Waveform of transition between the traditional normal mode and the Enhanced Eco-mode.(a) overall waveform (b) Zoomed-in waveform from traditional normal mode to the Enhanced Eco-mode.(c)Zoomed-in waveform from Enhanced Eco-mode to the traditional normal mode.

## *C. Transition between the traditional normal mode and the Burn-in test mode of the on-line UPS system*

*Case:1 No Load Condition.*

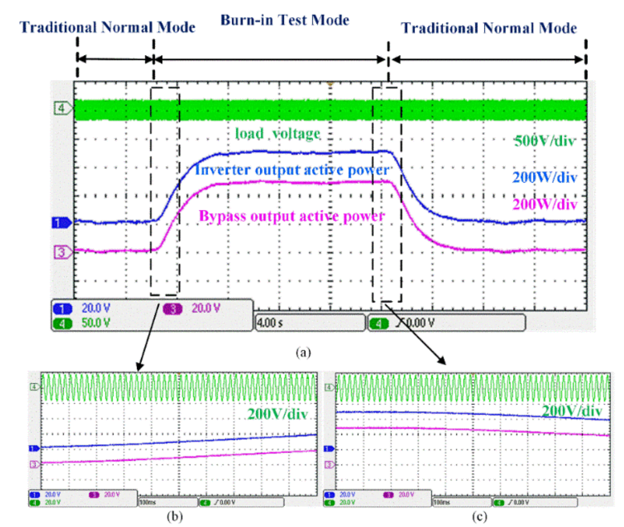

Fig.14. Waveform of transition between the traditional normal mode and the Burn-in test mode at no load condition.(a) overall waveform (b) Zoomed-in waveform from traditional normal mode to the Burn-in test mode.(c) Zoomed-in waveform from the Burn-in test mode to the traditional normal mode.

At no load condition, when the UPS system transfer its working mode from the normal mode to the burn-in test mode, the energy drawn by the inverter should be fed back into the grid. In case 1, the output active power of the inverter is set to be 500W (blue waveform). As no load is connected with the UPS system, the 500W of output active power is fed back into the grid through the bypass switch (Fig.14 (a)). Meanwhile, the load voltage during the transition is shown in Fig.14 (b) and (c), where it is observed that the seamless transition is realized as the output voltage has no abrupt change in voltage amplitude and frequency.

*Case:2 R-L Load is connected during the transition*

When the R-L load with 550W of active power and 120Var of reactive power connecting at the UPS system, as can be seen in Fig.15 that the inverter provides the load power. when the UPS system transfer its working mode from TNM to BTM, the active power drawn by the inverter is set to be 850W (blue waveform), the extra 300W of output active power is fed back into the grid through the bypass switch (Fig.15 (a) purple waveform). Meanwhile, the load voltage during the transition is shown in Figs.15 (b) and (c), where it is observed that the seamless transition is realized as the output voltage has no abrupt change in voltage amplitude and frequency.

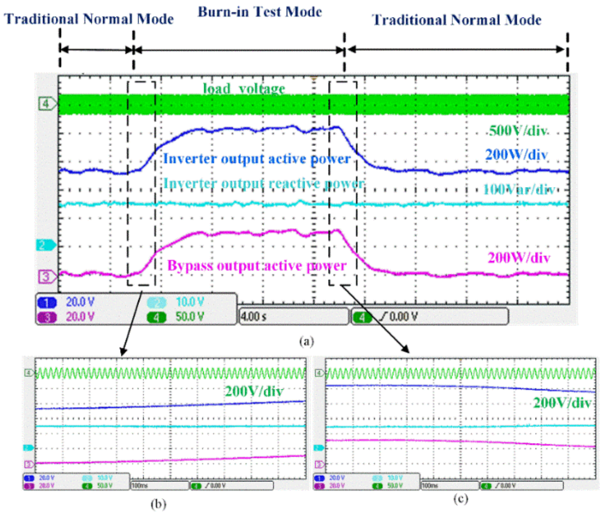


Fig.15. Waveform of transition between the traditional normal mode and the Burn-in test mode at R-L load condition.(a) overall waveform (b) Zoomed-in waveform from traditional normal mode to the Enhanced Eco-mode.(c)Zoomed-in waveform from Enhanced Eco-mode to the traditional normal mod

## V. Conclusion

In this paper, the multiple modes of operation for the on-line UPS system are proposed. First, some control strategies for PV-aided normal mode, Enhanced Eco-mode and Burn-in test mode are respectively presented to achieve the seamless transition in different modes of operation. With the application of these three mode, the cost charged from the grid can be greatly reduced. In addition, these modes of operation can be easily achieved by adjusting the reference value of the inverter in the on-line UPS system. The experimental results showed the effectiveness of the proposed control strategies.

## References

[1] M. S. Racine, J. D. Parham, and M. H. Rashid, "An overview of uninterruptible power supplies," in *Proceedings of the 37th Annual North American Power Symposium, 2005.*, 2005, pp. 159-164.

[2] G. N. Rajani, "Emerging trends in Uninterrupted Power Supplies: Patents view," in *2016 Biennial International Conference on Power and Energy Systems: Towards Sustainable Energy (PESTSE)*, 2016, pp. 1-5.

[3] "IEC_62040-3-2011 Uninterruptible power systems (UPS) –Part 3: Method of specifying the performance and test requirements."

[4] E. K. Sato, M. Kinoshita, Y. Yamamoto, and T. Amboh, "Redundant High-Density High-Efficiency Double-Conversion Uninterruptible Power System," *IEEE Transactions on Industry Applications,* vol. 46, no. 4, pp. 1525-1533, 2010.

[5] C. Zhang, J. M. Guerrero, J. C. Vasquez, and E. A. A. Coelho, "Control Architecture for Parallel-Connected Inverters in Uninterruptible Power Systems," *IEEE Transactions on Power Electronics,* vol. 31, no. 7, pp. 5176-5188, 2016.

[6] K. Shi, H. Li, C. Hu, and D. Xu, "Topology of super uninterruptible power supply with multiple energy sources," in *2015 9th International Conference on Power Electronics and ECCE Asia (ICPE-ECCE Asia)*, 2015, pp. 1742-1749.

[7] D. Dezhi, C. Linglin, L. Haijin, C. Min, and X. Dehong, "Design of hybrid AC-DC-AC topology for Uninterruptible Power Supply," in *2015 IEEE 2nd International Future Energy Electronics Conference (IFEEC)*, 2015, pp. 1-5.

[8] J. Zhou, H. Li, Z. Liu, C. Hu, and D. Xu, "Control strategy of Li-Ion Battery module in Super UPS," in *2014 International Power Electronics and Application Conference and Exposition*, 2014, pp. 1236-1241.

[9] W. Zhang *et al.*, "Seamless Transfer Control Strategy for Fuel Cell Uninterruptible Power Supply System," *IEEE Transactions on Power Electronics,* vol. 28, no. 2, pp. 717-729, 2013.

[10] N. Rasmussen, "Eco-mode:Benefits and Risks of Energy-saving Modes of UPS operation."

[11] M. Rascon, "Active Eco Mode in Single-Phase UPS," *White Paper*.

[12] L. Giuntini, "Active damping control of multi-mode UPS for power quality improvement," in *2015 17th European Conference on Power Electronics and Applications (EPE'15 ECCE-Europe)*, 2015, pp. 1-10.

[13] H. Shyh-Jier and P. Fu-Sheng, "Design and operation of burn-in test system for three-phase uninterruptible power supplies," *IEEE Transactions on Industrial Electronics,* vol. 49, no. 1, pp. 256-263, 2002.

[14] J. F. Chen, C. L. Chu, T. H. Ai, and C. L. Huang, "The burn-in test of three-phase UPS by energy feedback method," in *Power Electronics Specialists Conference, 1993. PESC '93 Record., 24th Annual IEEE*, 1993, pp. 766-771.

[15] C. L. Chu and J. F. Chen, "Self-load bank for UPS testing by circulating current method," *IEE Proceedings - Electric Power Applications,* vol. 141, no. 4, pp. 191-196, 1994.

[16] J. Lu, S. Golestan, M. Savaghebi, J. C. Vasquez, J. M. Guerrero, and A. Marzabal, "An Enhanced State Observer for DC-Link Voltage Control of Three-Phase AC/DC Converters," *IEEE Transactions on Power Electronics,* vol. PP, no. 99, pp. 1-1, 2017.

[17] J. M. Guerrero, L. Hang, and J. Uceda, "Control of Distributed Uninterruptible Power Supply Systems," *IEEE Transactions on Industrial Electronics,* vol. 55, no. 8, pp. 2845-2859, 2008.